EFFECT OF SYNTHESIS CONDITION AND ANNEALING ON THE

SENSITIVITY AND STABILITY OF GAS SENSORS MADE OF

Zn-DOPED γ-Fe$_2$O$_3$ PARTICLES

A Thesis

by

TAEYANG KIM

Submitted to the Office of Graduate Studies of
Texas A&M University
in partial fulfillment of the requirements for the degree of

MASTER OF SCIENCE

August 2009

Major Subject: Mechanical Engineering

EFFECT OF SYNTHESIS CONDITION AND ANNEALING ON THE

SENSITIVITY AND STABILITY OF GAS SENSORS MADE OF

Zn-DOPED γ-Fe$_2$O$_3$ PARTICLES

A Thesis

by

TAEYANG KIM

Submitted to the Office of Graduate Studies of
Texas A&M University
in partial fulfillment of the requirements for the degree of

MASTER OF SCIENCE

Approved by:

Chair of Committee,   Bing Guo
Committee Members,   Yongmei Jin
                         Xinghang Zhang
Head of Department,   Dennis O'Neal

August 2009

Major Subject: Mechanical Engineering

ABSTRACT

Effect of Synthesis Condition and Annealing on the Sensitivity and Stability of Gas

Sensors Made of Zn-Doped γ-Fe$_2$O$_3$ Particles. (August 2009)

Taeyang Kim, B.S., Korea Military Academy

Chair of Advisory Committee: Dr. Bing Guo

In this study, the effect of synthesis conditions and annealing process on the sensitivity and stability of gas sensors made of flame-synthesized Zn-doped γ-Fe$_2$O$_3$ particles was investigated.

Zn-doped γ-Fe$_2$O$_3$ particles were synthesized by flame spray pyrolysis using either H$_2$/Air or H$_2$/O$_2$ coflow diffusion flames. The particles were then annealed at 325~350˚C in a tube furnace under air atmosphere. Both as-synthesized and annealed particles were used as gas sensing materials to construct gas sensors. Transmission electron microscopy (TEM), X-ray diffraction (XRD), Brunauer-Emmett-Teller surface area measurement (BET), Williamson and Hall (WH) method were employed to characterize the particles. Gas sensors were fabricated by applying the as-synthesized and annealed particles on interdigitated electrodes. The response of the gas sensor to acetone vapor, H$_2$ in dry synthetic air was measured before and after three days of aging.

High-temperature flame (H$_2$/O$_2$) generated nanometer-sized particles; lower temperature flame (H$_2$/Air) generated micrometer-sized particles. Fe$_2$O$_3$ particles doped with 15% Zn showed the highest sensitivity. The sensors made from as-synthesized

particles showed a gas sensing sensitivity that was 20 times higher than the literature value. The sensors made of microparticles lost their sensing ability after three days of aging, but sensors made of nanoparticles did not show significant change after aging. Sensors made of annealed particles (either micro or nano) did not have significant gas sensing ability, but annealing process improved the stability of gas sensors. Analysis using the WH method showed that the microstrains decreased significantly in both H_2/O_2 and H_2/Air flame particles after annealing.

The results showed that sensors made of nanoparticles have higher gas sensing signal, and more resistant toward aging than sensors made of microparticles. In addition, annealing process affected on the stability favorably due to reduction of structural defects.

DEDICATION

To my God, lovely wife, Mira, precious daughter, Grace, and all of my family members who have always been there for me.

ACKNOWLEDGEMENTS

TABLE OF CONTENTS

LIST OF FIGURES

FIGURE   Page

LIST OF TABLES

1. INTRODUCTION

Gas sensors based on semiconductor metal oxides have been one of the most investigated devices of gas sensors. They have aroused the attention from many researchers interested in gas sensing due to their low cost, ease of fabrication, simplicity of use, and large numbers of detectable gases.[1]

Today, many companies, such as Figaro, FIS, MICS, UST, CityTech, Applied-Sensors, NewCosmos, provide metal oxide based gas sensors. Their applications range from detection of combustible or toxic gas, to air intake control in automobile, and to glucose biosensors.[2]

Even though many different metal oxides have been investigated as gas sensor materials, gamma-iron oxide (γ-Fe$_2$O$_3$) is an n-type semiconductor and one of the most commonly used materials in research due to many merits, such as high sensitivity, low cost, quick response and low power consumption.[3] Tao et al.[4] reported that gas sensitivity of γ-Fe$_2$O$_3$ to alcohol was greatly improved by doping Y$_2$O$_3$ through sol-gel process. Jing[5] promoted the sensitivity and selectivity of γ-Fe$_2$O$_3$ towards acetone, ethanol, methane, and hydrogen by doping it with Ni. Z. Jiao et al.[6] enhanced the selectivity and stability of gas sensor to acetone, H$_2$, CO and CH$_4$ by using SnO$_2$/Fe$_2$O$_3$ multilayer thin film. Yamazoe[7] proposed two types of sensitization mechanism for various dopant materials; chemical sensitization, electronic sensitization.

This thesis follows the style of Materials Science and Engineering B.

Gas sensors should provide long-term performance, even at high operation temperature and in harsh environment. In general, any gas sensing device should exhibit a stable and reproducible signal for the period of at least 2 – 3 years.[8] The requirement means that stability of gas sensor is one of the most important factors determining the practical use of gas sensors.

Many parameters affect the stability of a gas sensor, such the grain size of sensing material (synthesis method), reducing gas, operating temperature, relative humidity, annealing process, film thickness, and deposition method.[9] This study focused on some of these parameters (grain size of sensing material, reducing gas, operating temperature, annealing process) to determine the effect of synthesis conditions and annealing process on the sensitivity and stability of gas sensors made of flame-synthesized Zn-doped Fe_2O_3 particles before and after 3-day aging.

2. THEORY

Gamma-Fe_2O_3 based gas sensor detects gases via variations in their resistances. Oxygen electron vacancies in the γ-Fe_2O_3 particles operate as donors, so provide free charge carriers that transfer oxygen gas to the negative charged oxygen adsorbates, which play important role in detecting inflammable gases such as acetone, H_2 and CO. Oxygen adsorbates, such as O^-, is known to cover the surface of semiconductor metal oxides in air and eventually the variation in surface coverage of O^- dominates the sensor resistance.[10]

Sensor selectivity and rate of target gas absorption are influenced by reactions between the sensing material surface and the target gas. These reactions are in turn, affected by catalysts on the material surface, ambient conditions, and sensor temperature. When thermal energy is supplied to γ-Fe_2O_3 particles, the free charge carriers (electrons for γ-Fe_2O_3) increase and cause a decrease in resistance. Then synthetic air is supplied, the free charge carriers are absorbed by O_2 gas. So the surface of γ-Fe_2O_3 acts as an electric potential barrier which decreases conduction between particles. Finally, Reducing gases, many of which combustible gases, are supplied, oxygen adsorbates on the γ-Fe_2O_3 surface are removed by combining with reducing gases. This causes the free charge carriers captured in oxygen adsorbates to move into γ-Fe_2O_3 nanoparticles; which weakens the electric potential barrier and increases particle conduction. These processes can be explained by following equations.

$$S + e^- + \frac{1}{2}O_2 \leftrightarrow S - O_s^- \qquad (1)$$

$$S - O_s^- + R \rightarrow RO + e^- + S \qquad (2)$$

Where S denotes a surface adsorption site, e^- is a free electron, R is a reducing gas, such as H2, CO, C_3H_5O, and $S-O_s^-$ is an oxygen adsorbates. The reversible reaction (1) is affected by temperature and oxygen partial pressure.[11]

As a result, the rate of adsorption and desorption of oxygen is a key factor that affects the sensor's sensitivity to various gases.

3. METHODOLOGY

3.1 Equipment

Flame spray pyrolysis apparatus, Thermolyne® Type 1900 Hot Plate(Sigma – Aldrich, St.Louis, MO), Thermolyne® 21100 Tube Furnace(Barnstead International, Dubuque, Iowa), Multi Gas Controller 647c (MKS Instrument, Andover, MA), 6485 Picoammeter (Keithley, Cleveland, OH), Digital Triple Output DC power supply (Extech Advantage, Waltham, MA), Omega Engineering HHM28 (OMEGA Engineering, Stamford, CT), Ultrasonic Cleaner (VWRInternational, Arlington ,IL), Interdigitated Finger Electrode with heater and temperature detector (Case Western Reserve University, Cleveland, OH), Alumina Filter (Whatman, Maidstone, England), syringe pump (Cole Parmer, Vernon Hills, IL) and the gas chamber.

3.2 Flame Spray Pyrolysis Apparatus

Zn-doped γ-Fe$_2$O$_3$ sensor materials were prepared by flame spray pyrolysis method using H$_2$ diffusion flame with O$_2$ or air support. Figure 1 shows a schematic of the flame spray pyrolysis apparatus. The precursor solution was injected at a steady flow rate (5 ml/hr) into the atomizer vessel using a syringe pump (Cole Parmer, Vernon Hills, IL). The H$_2$ fuel gas flew through the vessel and carried the precursor droplets generated by atomizer into the flame through the furnace. The droplets underwent solvent evaporation and precursor decomposition to form Zn-doped γ-Fe$_2$O$_3$ particles. The H$_2$ and O$_2$ (or Air) flow rates were kept at 1 SLM and 6 SLM respectively. Zn-doped γ-Fe$_2$O$_3$ particles then were collected on an alumina filter (Whatman, Maidstone, England). The flame spray pyrolysis method had been described in detail elsewhere [12].

The precursor solution was prepared by dissolving Zn(NO$_3$)$_2$·6H$_2$O (Zinc(III) nitrate hexahydrate, 99.9%, Alfa Aesar) and Fe(NO$_3$)$_3$·9H$_2$O (Iron(III) nitrate nonahydrate, 99.9%, Alfa Aesar) in deionized (DI) water. The molar concentration of the solution was 0.75 M(mol/L) in terms of total metal ions, with various Zn/Fe atomic ratios from 0/100 to 100/0.
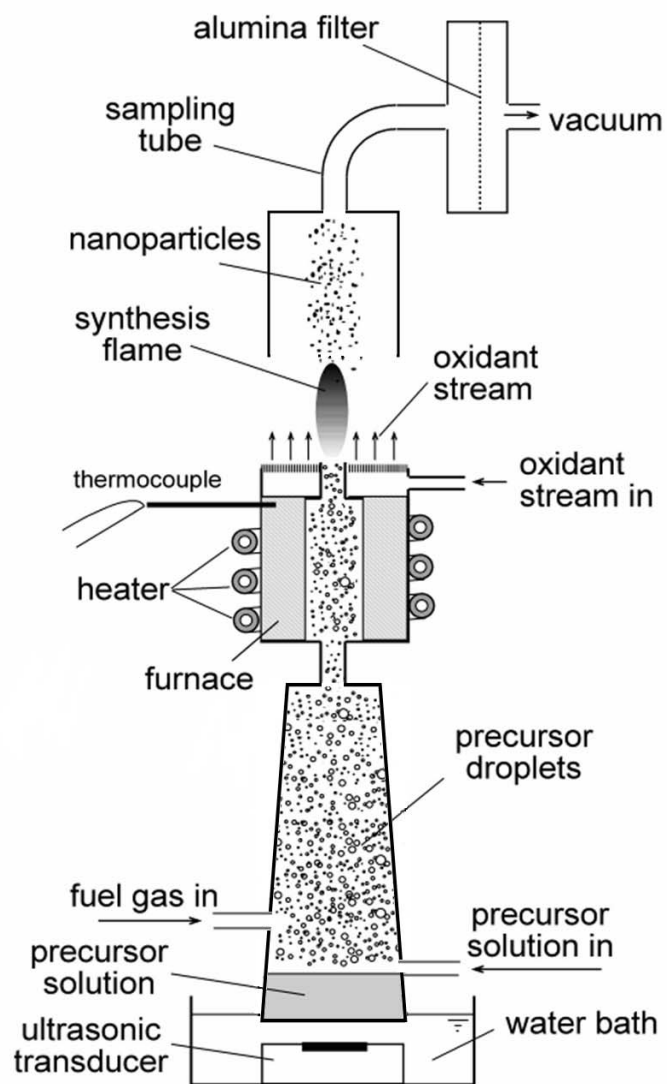
Figure 1. Schematic of flame spray pyrolysis apparatus

3.3 Gas Sensing Apparatus

Zn-doped γ-Fe$_2$O$_3$ particles were suspended in DI water. Sonication with an Ultrasonic Cleaner (VWR International, Arlington, IL) was used to disperse the particles. The DI water suspension of the Fe$_2$O$_3$ particles was applied drop-wise on the interdigitaged electrodes (Case Western Reserve University, Cleveland, OH) to make the gas sensors. Heating the sensor to approximately 150°C greatly enhanced the speed at which the DI water evaporated; leaving behind a coating of Zn-doped γ-Fe$_2$O$_3$ particles. Figure 2 shows how the gas chamber, picoammeter, power supply, bubbler, and mass flow controller were physically connected throughout the experiments. The gas chamber consisted of an inlet, an outlet, holder for gas sensor and 7 signal/power connectors linked to electrode. Figure 3 is an illustrative representation of the gas chamber. The experiment was designed to change only the electrode temperature, target gas, and target gas concentration. Background gas, background gas flow rate, and electrode voltage were kept constant in all experiments.
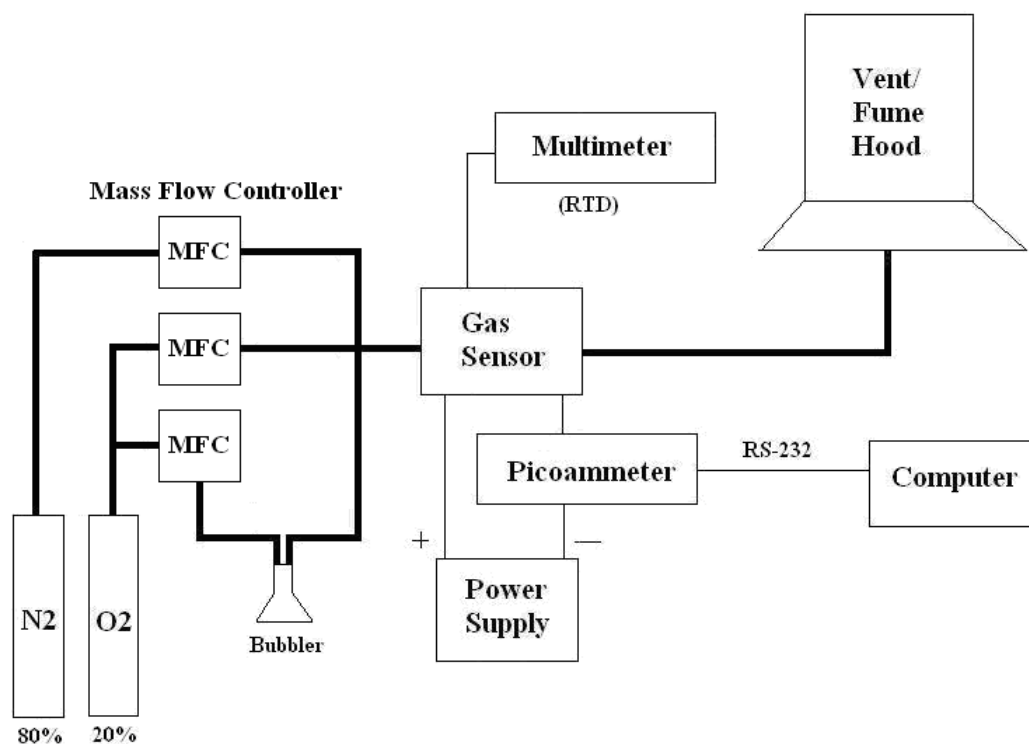
Figure 2. An illustrative representation of the experimental setup
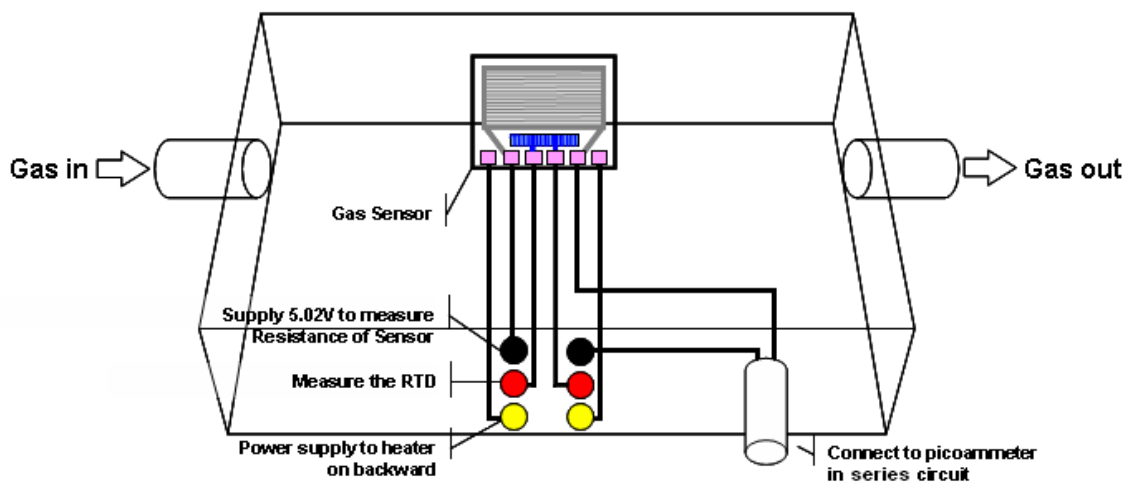
Figure 3. A schematic representation of the gas chamber

First, the initial Resistance Temperature Device (RTD) resistance was measured at room temperature without a gas flow. Equation (3) is the calibrated resistance to temperature curve for the RTD with an R^2 value of 0.9967.

$$T_{Heater} = 56.21 * R_{RTD} - 241.4 \qquad (3)$$

The electrode temperature was controlled by the power of the heater on the opposite side of the electrode. If at any point the temperature of the electrode fell or rose above the desired temperature, then the power input to the heater was adjusted accordingly to maintain the operating conditions. Figure 4 is an illustrative representation of the electrode.

Figure 4. Illustrative representations of the platinum interdigitated electrodes

3.4 Sensor Signal Measurement

Target and background gas flow was controlled by the mass flow controller and their ratio is calculated using partial pressures. Acetone gas was generated by passing oxygen gas through liquid acetone in the bubbler. Measurements during experiments were taken after at least 10 minutes of Synthetic air flow only to remove diffusion effect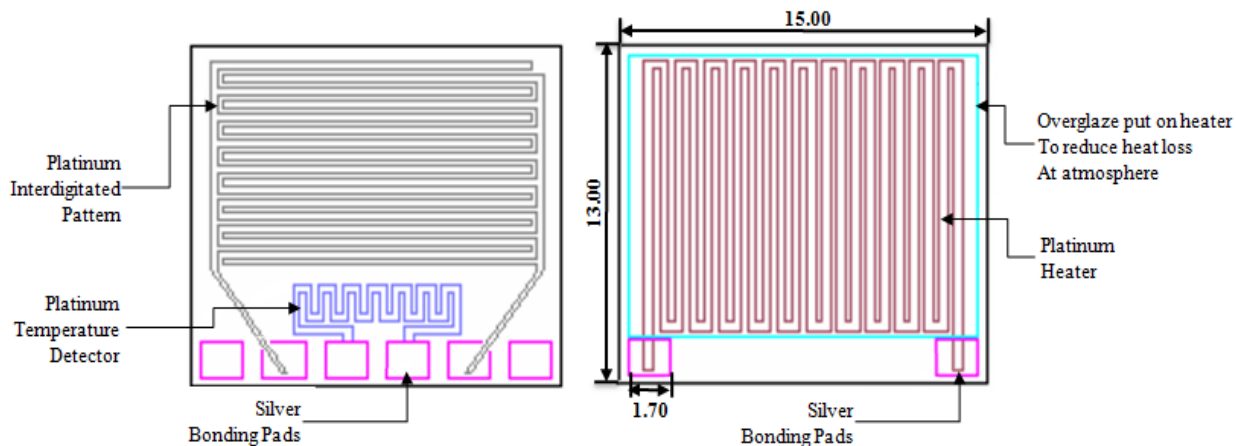s between the sensor material and previous target gas. Synthetic air was used as the background gas to minimize humidity effect of the gas. Table 1 displays all the flow rates for background gas and the target gasses corresponding to desired concentration.

Table 1. Flow rates of target gases and Synthetic air

Target Gas	Acetone Vapor				H_2			
Concentration (ppm)	250	500	750	1000	500	1000	1500	2000
Synthetic Air (SLM)	4SLM (N_2:3.2 SLM, O_2:0.8 SLM)				4SLM (N_2:3.2 SLM, O_2:0.8 SLM)			
Flow rate(sccm)	3.6	7.2	10.8	14.5	2	4	6	8

Since target gas concentration was a major factor in the rate of adsorption, an accurate method of calculating target gas concentration was needed. Using partial pressures and the saturation vapor pressure of the target gas (acetone), the acetone gas was introduced into the main 4 SLM flow of synthetic air via a bubbler. This

assumption was valid for small flow rates because the gas can get the sufficient residence time in the bubbler to forms separate bubbles only at small flow rates and at large flow rates, a gas jet was formed i.e. less than 100 SCCM. And H_2 gas was injected into the main 4 SLM flow of synthetic air directly. Synthetic air was used in the experiments to minimize the influence of humidity.
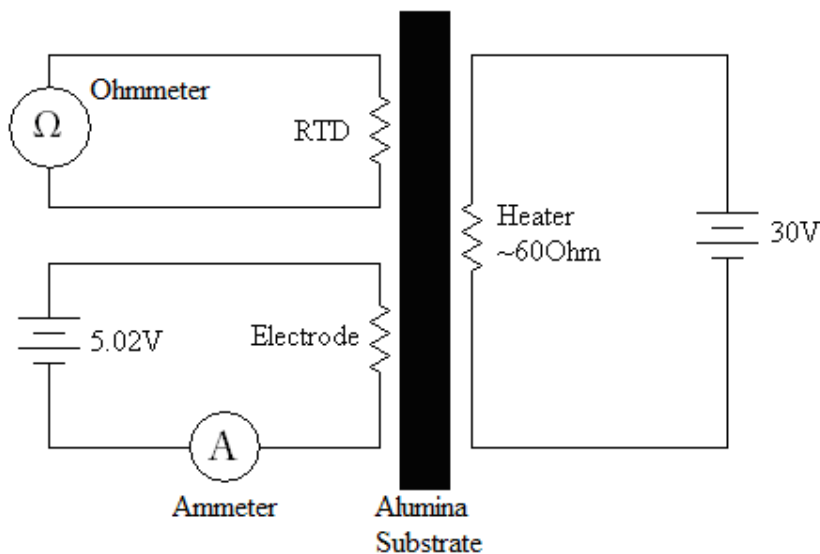
Figure 5. Illustrative representation of the electrical circuitry

Figure 5 shows how the connections were created and the quantities measured. Resistance of the RTD was measured using the ohmmeter setting on a multimeter. During the gas sensing experiment, the resistance of the RTD was monitored with Omega Engineering HHM28 multimeter (OMEGA Engineering, Stamford, CT) to ensure that the gas sensor temperature was constant within $\pm$ 5.5 ˚C. The picoammeter

was connected in series with the sensing material to measure the current across the materials. A voltage of 5.02 was applied across the sensing material to effectively turn the sensing material into a resistor. Equations (4) and (5) show how the current from the picoammeter was converted into the sensor signal. The sensor signal was defined as the ratio of the sensing material's electrical resistance in the background gas, R_b, to the sensing material's electrical resistance in the present of target gas, R_t.

$$S_{signal} = \frac{R_b}{R_t} \qquad (4)$$

$$R_{Material} = \frac{V_{Electrode}}{I_{Picoammeter}} = \frac{5.02V}{I_{Picoammeter}} \qquad (5)$$

The sensing material's electrical resistance was calculated from the voltage applied on sensor and the current measured with the picoammeter. The picoammeter read/recorded the current once every 2 seconds.

3.5 Sensor Stability Measurement

Figure 6 shows the model indicates variables and results used to acquire the stability. The stability was defined as the ratio of the signal of after aging to the signal of before aging.
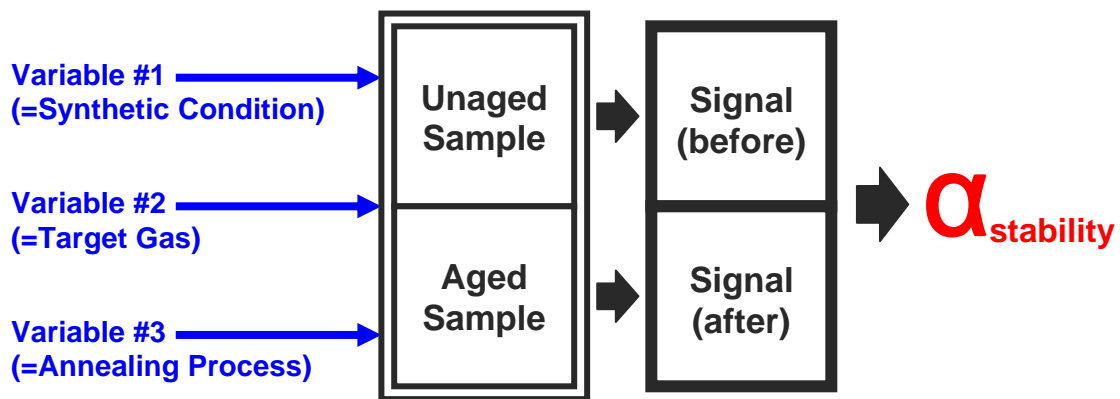
Figure 6. Illustrative representation of the stability model

$$\alpha_{Stability} = \frac{S_{after}}{S_{before}} \tag{6}$$

Annealing was carried out by leaving Zn-doped Fe_2O_3 particles on the glass plate in the tube furnace for 3 days, while maintaining existence of ambient air and inside furnace temperature at 325°C for H_2/Air flame particles (350°C for H_2/O_2 flame)using Thermolyne® 21100 Tube Furnace (Barnstead International, Dubuque, Iowa).

3.6 Characterization

Following equipments and method were used to characterize the properties of particles.

X-ray Diffraction (XRD)

The particles collected on alumina filter were directly put on the sample stage and analyzed in a Bruker-AXS D8 Powder X-ray diffractometer (Bruker, Madison, WI) with Cu source.

Transmission Electron Microscopy (TEM)

For the transmission electron microscopy (TEM) analysis, Zn-doped γ-Fe$_2$O$_3$ particles were carefully scraped off the filter and suspended in ethanol. Drops of the Zn-doped γ-Fe$_2$O$_3$ ethanol suspension were put on 300 mesh copper grids with type-B carbon film support (Ted Pella Inc., CA). After evaporation of the ethanol, Zn-doped γ-Fe$_2$O$_3$ particles were deposited on the grids and TEM samples were thus obtained. Transmission electron microscopy (TEM) samples were then measured in a JEOL 2010 microscope (Jeol Ltd., Tokyo, Japan) operated at 200kV. The TEM images were recorded with a Gatan ORIUS CCD camera (Gatan Inc., Pleasanton, CA).

Williamson and Hall Method

Williamson and Hall(WH) method[13] was used to determine the quantity of microstrains of Zn-doped γ-Fe_2O_3 particles before and after annealing. It suggested that line broadening was attributed to simultaneous small particle size and microstrains, the latter predominating, particularly at higher Bragg angles. Peaks of particles before and after annealing were analyzed with XRD data and following equations were used for determining the mean microstrains.

$$\beta^* = \beta \cos\theta / \lambda \tag{7}$$

$$d^* = 2\sin\theta / \lambda \tag{8}$$

where β^* is reciprocal peak breadth, β is integral breadth(peak area/maximum intensity), Θ is Bragg angle, λ is X-ray wavelength, d^* is reciprocal lattice distances. As a result, mean microstrains of particles was calculated by plotting β^* versus d^* in which slope of fitted lines represents the mean microstrains.

4. RESULTS AND DISCUSSION

4.1 Particle Size and Morphology

Figure 7 shows representative TEM images of Zn-doped γ-Fe_2O_3. Particle sizes of Zn-doped γ-Fe_2O_3 formed in H_2/O_2 diffusion flame are much smaller than ones formed in H_2/Air diffusion flame. Adiabatic temperature of H_2/O_2 diffusion flame is about 2700 ℃ and H_2/Air diffusion flame is about 2100 ℃. That is, high-temperature flame generated nanometer-sized particles; lower temperature flame generated micrometer-sized particles.

It can be explained by melting temperature of iron oxide particles. Melting temperature of iron oxide is 1566 ℃, so iron oxide exists as liquid phase in the both flame. However, especially in H_2/O_2 diffusion flame, more portion of iron oxide particles would exist as gas phase than ones formed in H_2/Air diffusion flame. As a result, lower-sized particles could be accepted in H_2/O_2 diffusion flame.
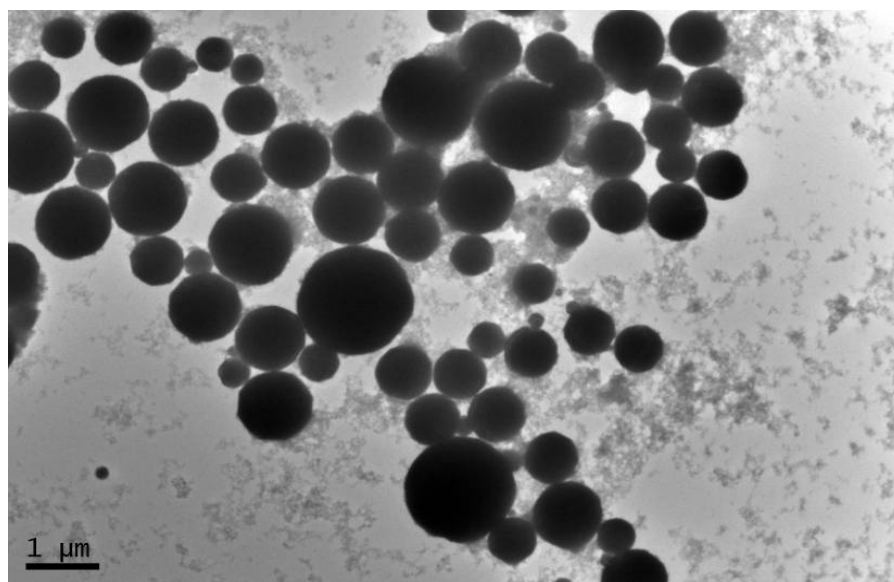
(a)
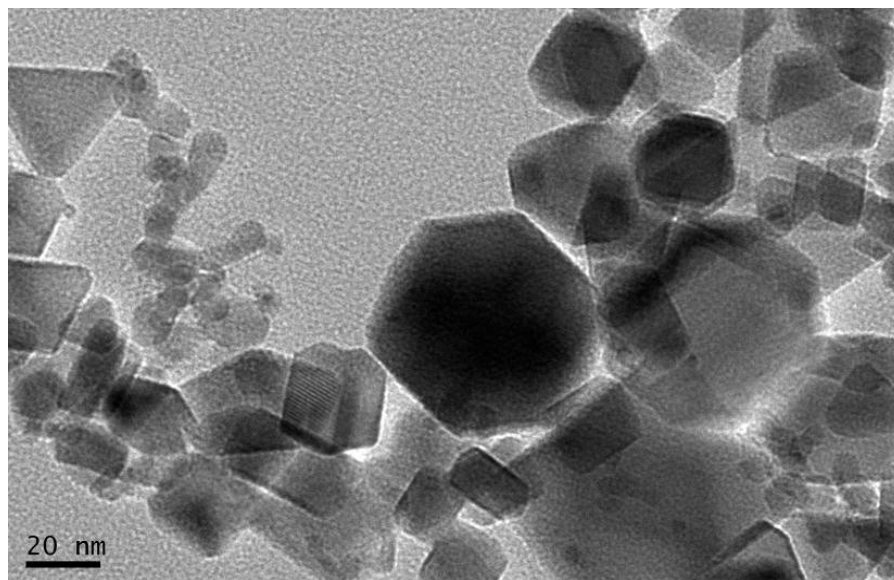
(b)

Figure 7. Representative TEM images of Zn-doped γ-Fe$_2$O$_3$ (a) in H$_2$/O$_2$ diffusion flame and (b) in H$_2$/Air diffusion flame

4.2 Signal of Gas Sensor

The signals of various gas sensors made of different concentrations of Zn doped (undoped, 15%, 30%, 50%, 100%) γ-Fe_2O_3 particles are shown in Figure 8. 15 % Zn doped γ-Fe_2O_3 particles showed the highest signal to both target gases. As a result, 15% Zn dopant is an optimal concentration to detect acetone vapor and H_2 gas.
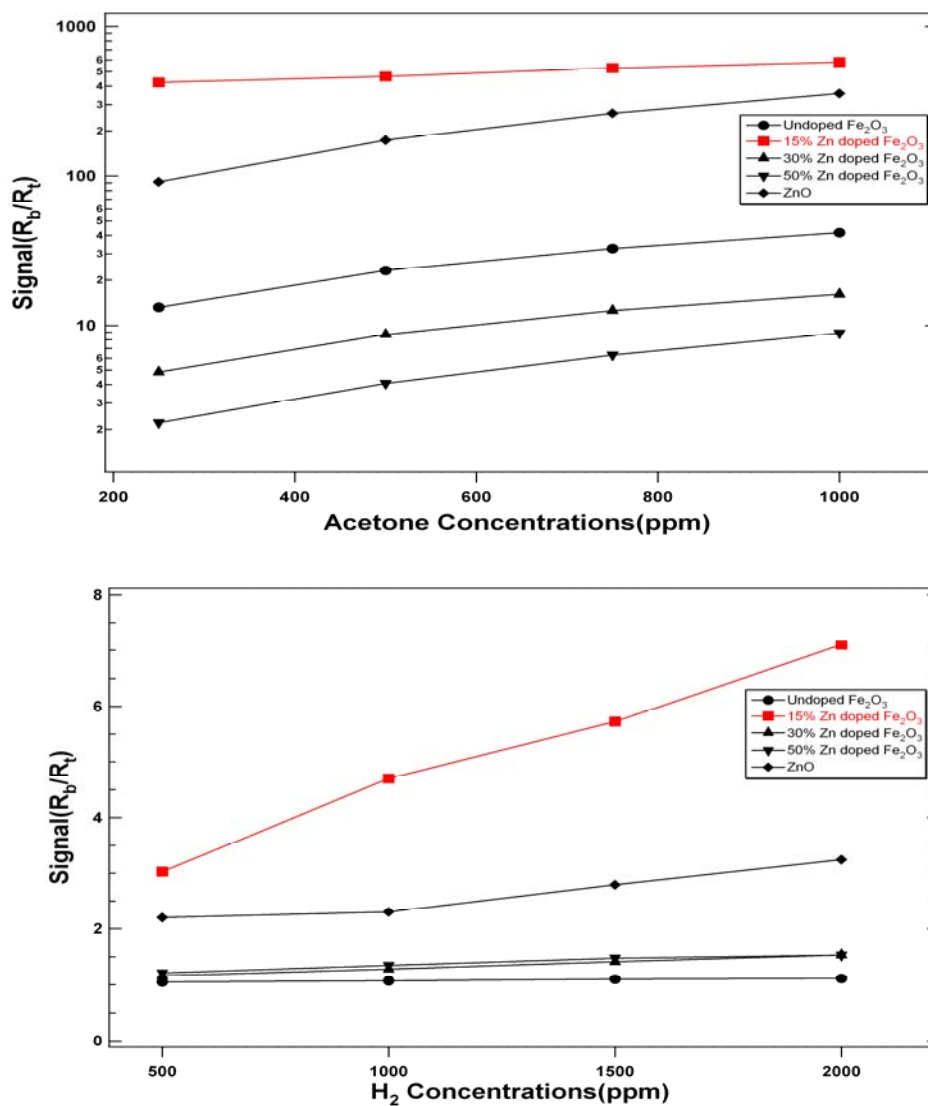
Figure 8. Signal of γ-Fe_2O_3 gas sensors with various Zn dopant concentrations; to acetone (above) and H_2 gas (below)

Figure 9 shows representative TEM images of various concentration of Zn-doped γ-Fe$_2$O$_3$ made from H$_2$/O$_2$ flame. There was no significant change in morphology and particle size between samples except for ZnO particles which have nanorod morphology and bigger particle size.

Figure 9. TEM images of various concentrations Zn doped Fe2O3 formed in H$_2$/O$_2$ flame; (a) Undoped, (b) 15% doped, (c) 30% doped, (d) 50% doped, (e) 100% doped; ZnO

Figure 10 shows how the sensor signals towards acetone of Zn-doped γ-Fe$_2$O$_3$ particles synthesized using H$_2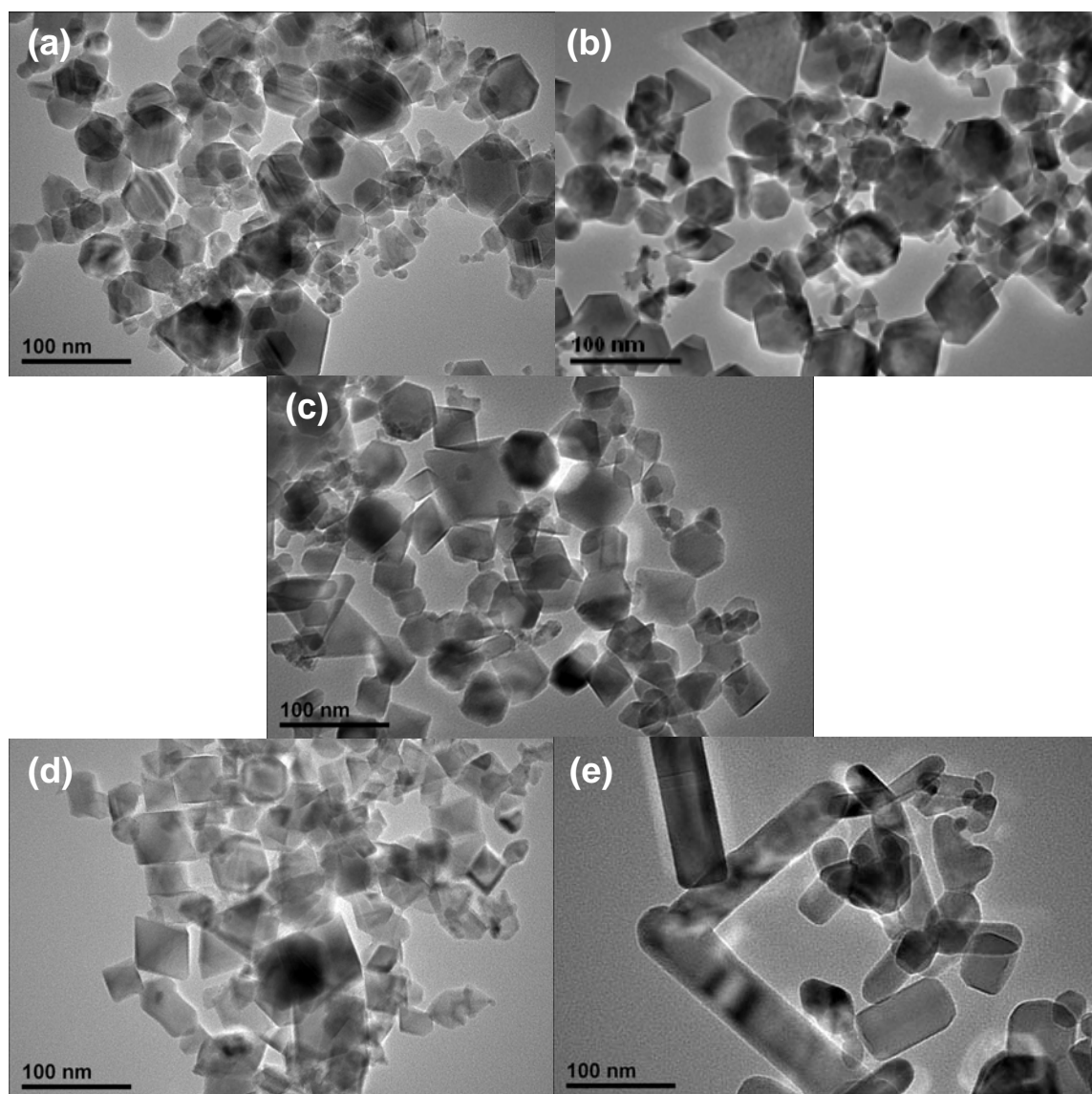$/Air and H$_2$/O$_2$ flames. The two temperatures tested were chosen due to their high signal strength at 1000ppm acetone.
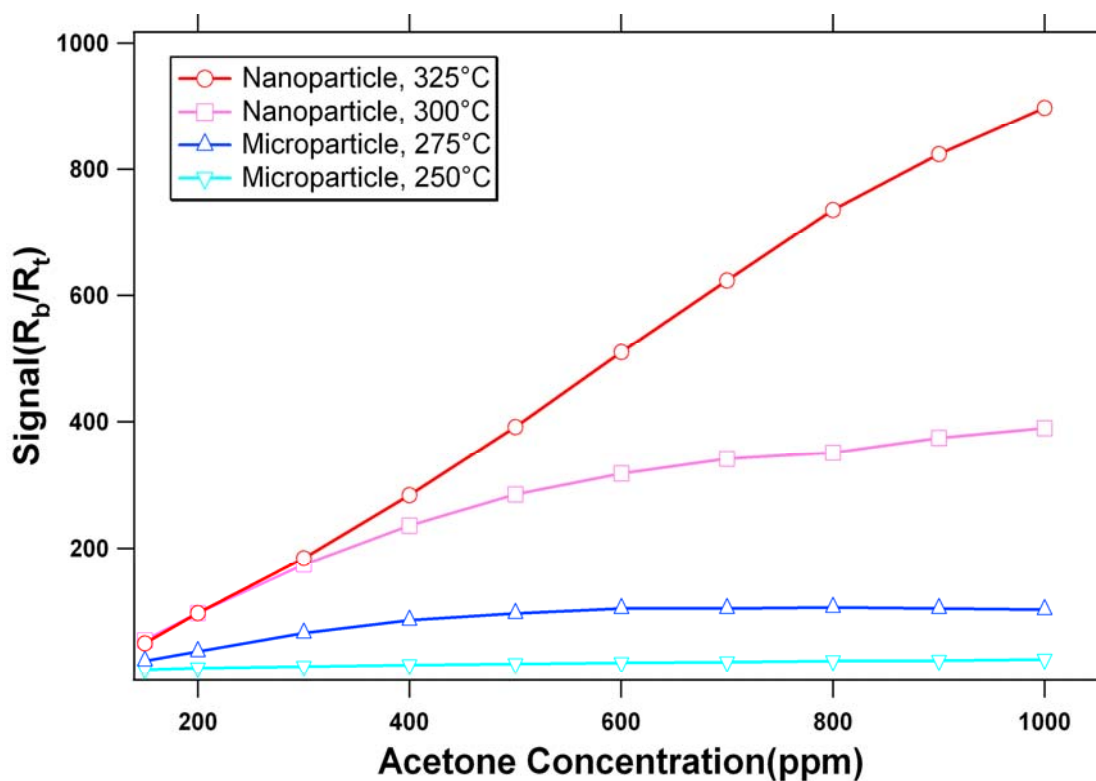
Figure 10. Signal of gas sensors made of particles from H$_2$/O$_2$ and H$_2$/Air flames as a function of acetone concentrations and sensor temperatures

The sensors made from nanoparticles showed higher gas sensing sensitivity than sensors made of microparticles, which can be explained by surface area-volume ratio of particles.[14] According to BET measurement, BET surface area of H$_2$/O$_2$ flame, as-synthesized particles is 10.4849m^2/g and BET surface area of H$_2$/Air flame, as-synthesized particles is 2.8387m^2/g. The amount of oxygen adsorbates per volume of

Zn-doped γ-Fe$_2$O$_3$ particles increases with decreasing particle size, causing a further increase in resistance at small particle size.[10]

The signals for various target gases and processing methods before and after aging were shown in Figures 11 and 12. The sensors made from H$_2$/O$_2$ flame, as-synthesized particles showed the highest gas sensing ability. The sensors made of H$_2$/Air flame particles lost their sensing ability after three days of aging, but sensors made of H$_2$/O$_2$ flame particles did not show significant change after aging. However, the sensors made of annealed particles, either micrometer-sized and nanometer-sized, did not show significant gas sensing ability. Tables 2 and 3 display the signals towards 1000ppm target gas concentration of sensors made of various particles.

Table 2. Signal of sensors made of various particles towards 1000 ppm acetone

	H$_2$/O$_2$ Flame particles		H$_2$/Air Flame particles	
	As-synthesized	annealed	As-synthesized	annealed
Signal unaged	701.4	3.85	530.9	3.26
Signal aged	831.53	7.1	15.15	2.16

Table 3. Signal of sensors made of various particles towards 1000 ppm H$_2$

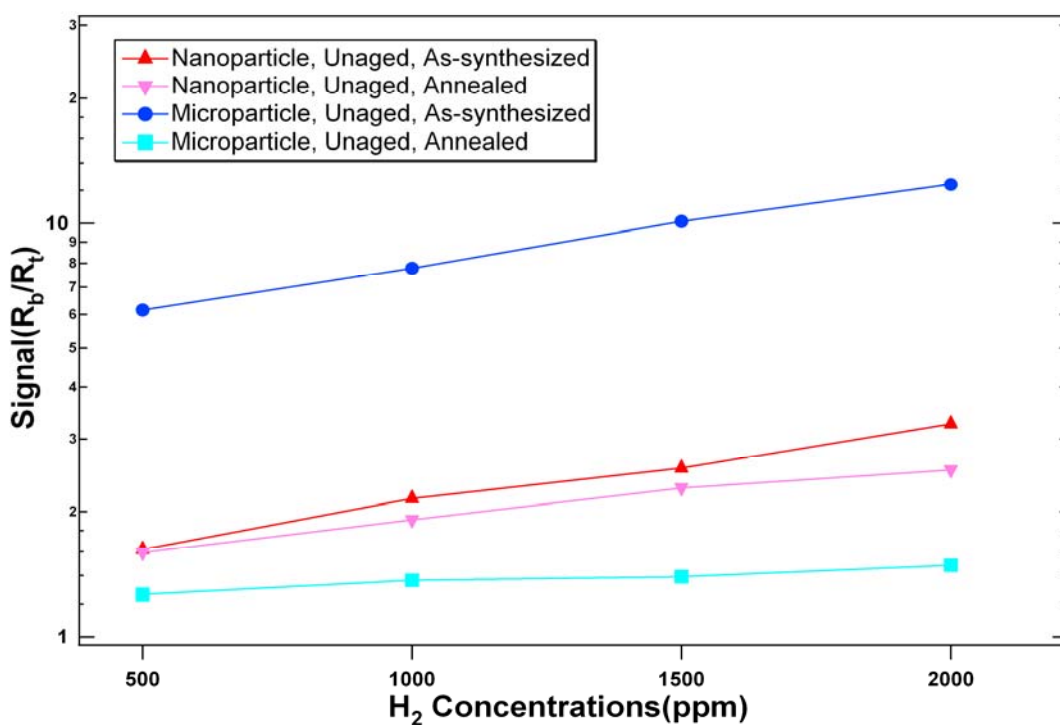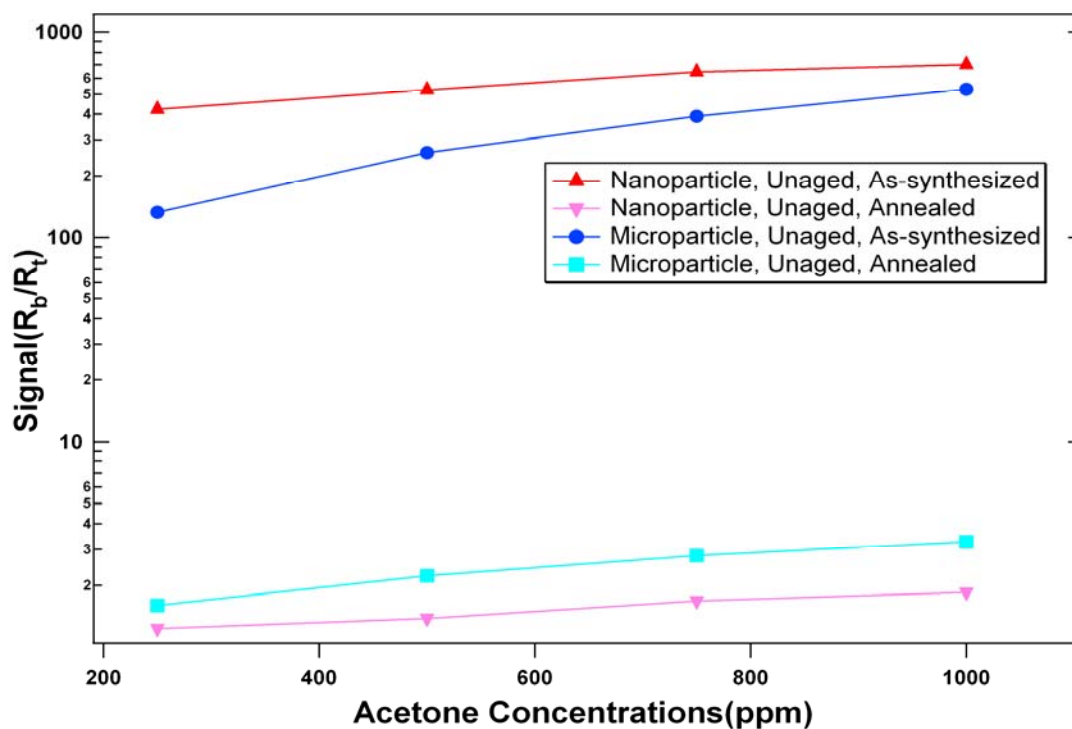|	H$_2$/O$_2$ Flame particles		H$_2$/Air Flame particles	
	As-synthesized	annealed	As-synthesized	annealed
Signal unaged	2.522	3.256	12.41	1.483
Signal aged	3.464	5.427	1.649	1.034

Figure 11. Signal of gas sensors made of nanoparticles and microparticles before and after annealing; to the acetone vapor (above) and H$_2$ gas (below)
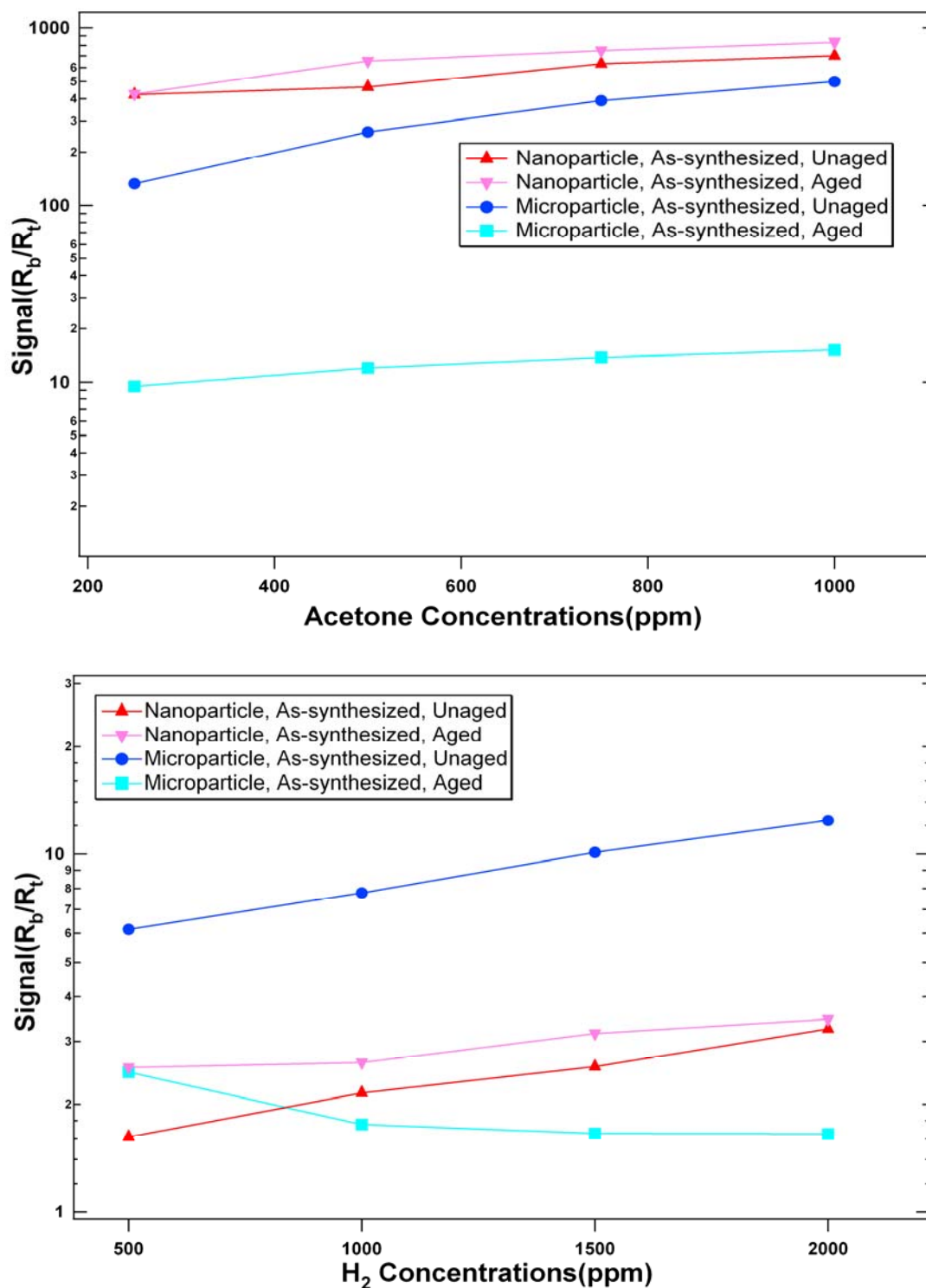
Figure 12. Signal of gas sensors made of nanoparticles and microparticles before and after aging; to the acetone vapor (above) and H_2 gas (below)

4.3 TEM Analysis

Figure 13 shows representative TEM images of Zn-doped γ-Fe₂O₃ made from different synthesis conditions before and after annealing. It proved that the particle size and morphology didn't have significant change after annealing process, so that reduction of sensor ability after annealing was not because of change of particle size and morphology.
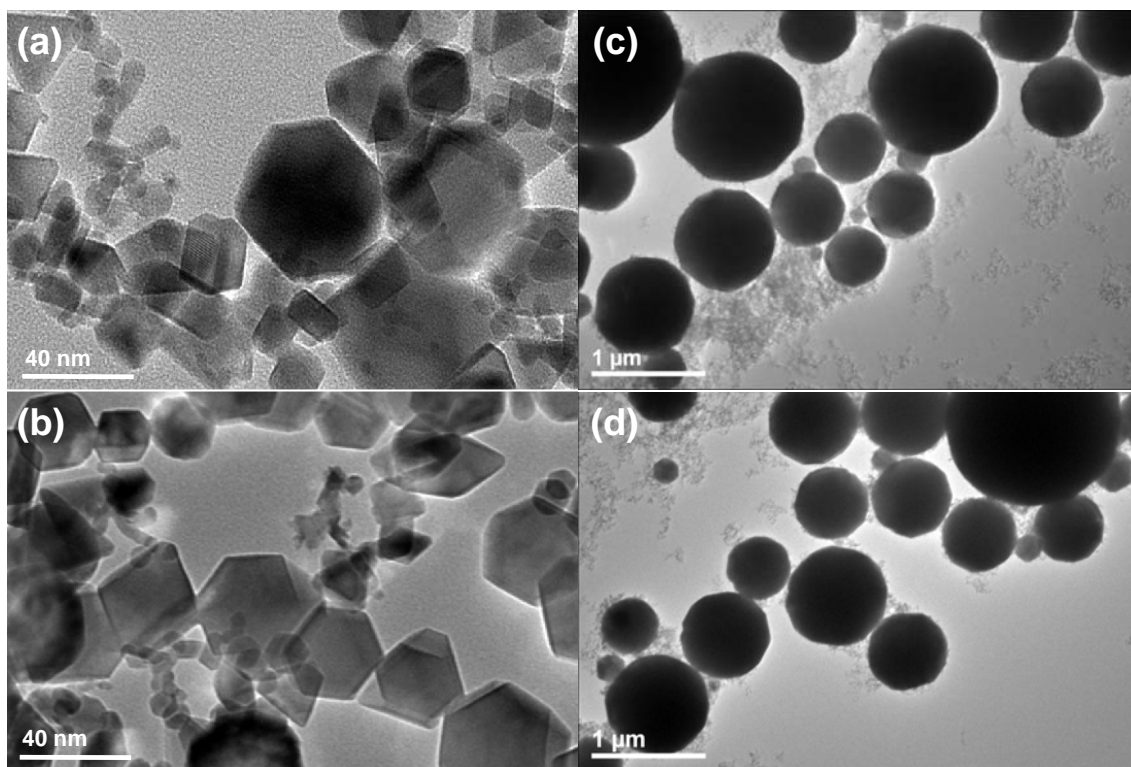
Figure 13. TEM images of Zn-doped γ-Fe₂O₃; formed in (a) H₂/O₂ diffusion flame, As-synthesized, (b) H₂/O₂ diffusion flame, Annealed, (c) H₂/Air diffusion flame, As-synthesized and (d) H₂/Air diffusion flame, Annealed

Particle size distributions for different particles are shown in Figure 14. There was no significant difference in size distribution between the as-synthesized and annealed particles made in both flame. It supported the fact that annealing process didn't affect on the change of particle size.
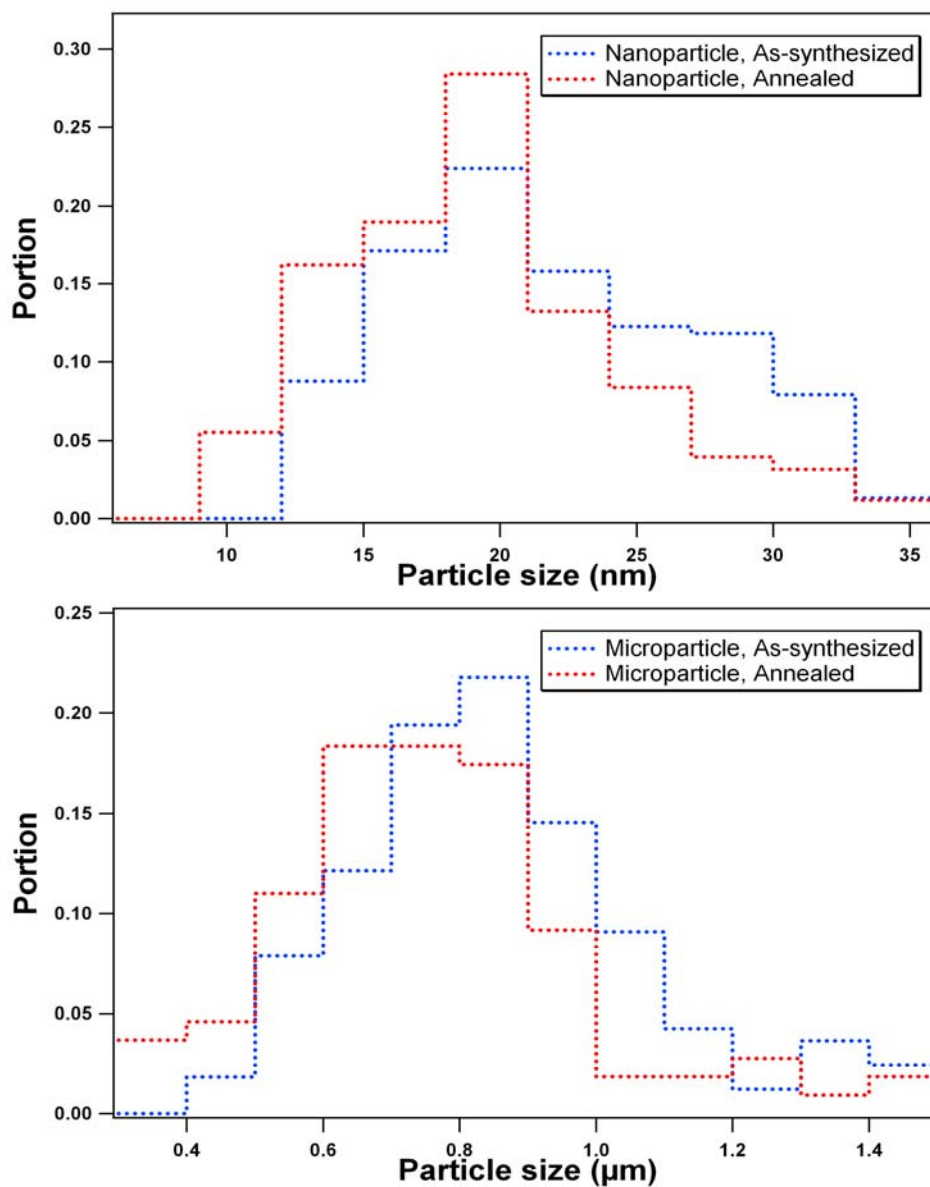
Figure 14. Particle size distribution for different samples; nanoparticles(above) and microparticle(below)

4.4 XRD Analysis

Crystalline structure of Zn-doped γ-Fe$_2$O$_3$ particles with various synthesis conditions and processing was shown in the figure 15; PDF#39-1346 (Maghemite). It indicates the crystalline structure of Zn-doped γ-Fe$_2$O$_3$ particles made of H$_2$/Air and H$_2$/O$_2$ diffusion flames was not changed before and after annealing, so that deterioration of sensor ability after annealing was not because of change of crystalline structure.
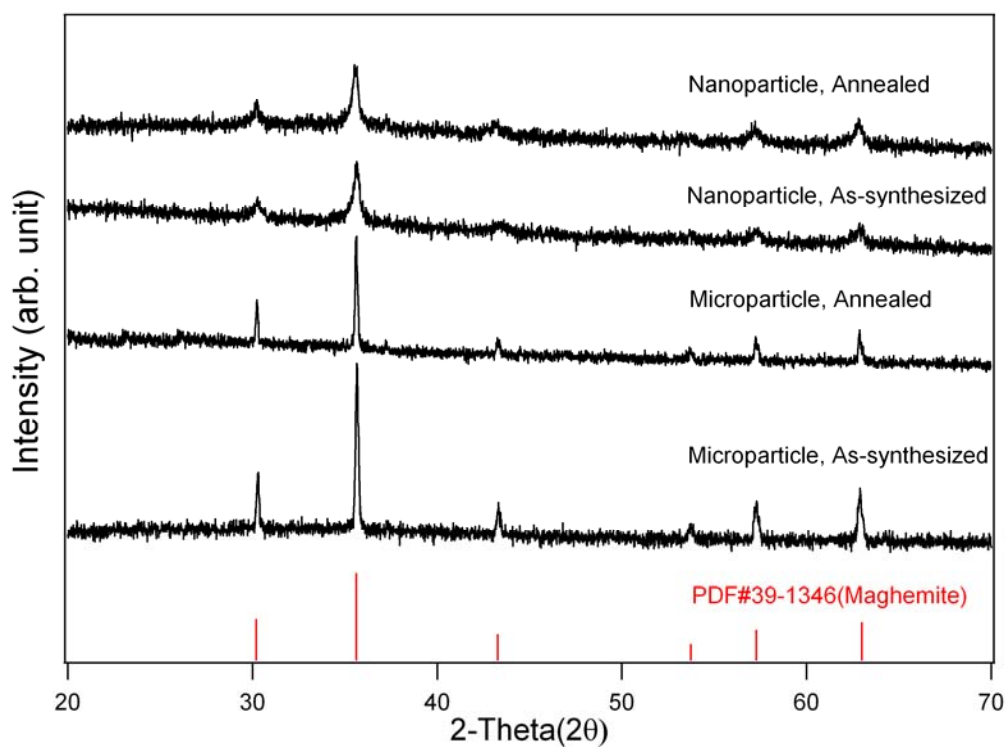
Figure 15. XRD data for Zn-doped γ-Fe$_2$O$_3$ particles made of H$_2$/Air and H$_2$/O$_2$ diffusion flames before and after annealing

4.5 Microstrain Analysis: WH Method

Figure16 showed the change of mean microstrains of different sample before and after annealing. The slope of fitted lines decreased two or three times after annealing in H_2/O_2 flame sample, H_2/Air flame sample, respectively. That is, annealing process has a major effect on improving the lattice quality, reducing point and line defects to a very low level.[15]

In conduction mechanism of metal oxide semiconductor, oxygen vacancy operates as donor, provides free charge carriers to transfer oxygen gas to negative charged oxygen adsorbates which play important role in determining the signal of gas sensor. And oxygen vacancy is a kind of point defect. Lattice defects, such as dislocations, can either trap or provide extra free electrons.[16] Therefore, we can conclude that one of the possible causes of the reduction in the signal after annealing is associated with the reduction of defects in the Zn-doped Fe_2O_3 layer.

Figure 16. WH plot of different sample before and after annealing

4.6 Stability of Gas Sensor

The stability for various target gases and processing methods was shown in the figure 17.
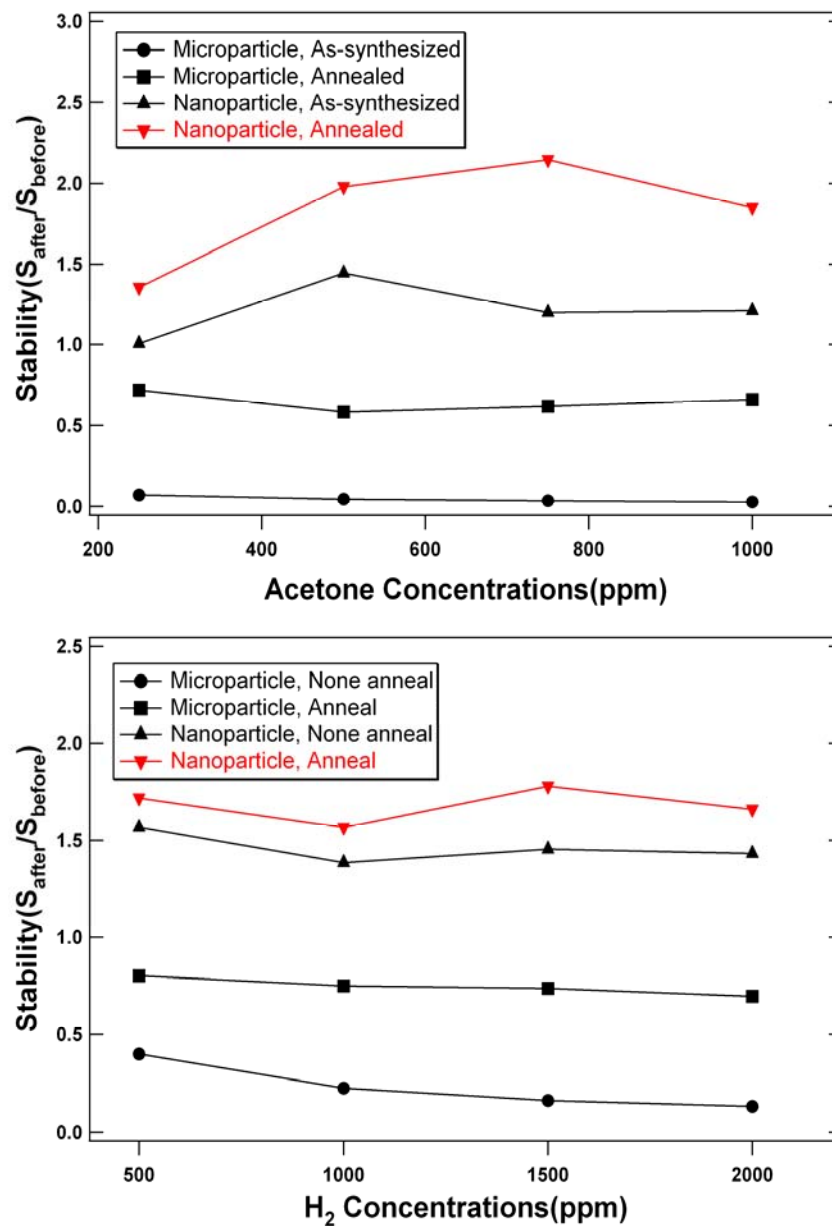
Figure 17. Stability of gas sensors made of H_2/O_2 and H_2/Air flames, as-synthesized and annealed particle; to the acetone vapor (above) and H_2 gas (below)

In all target gases, the sensors made of H_2/O_2 flame particles had higher stability than one made of H_2/Air flame particles. And annealing processing promoted the stability of gas sensors. As a result, the synthesis condition using H_2/O_2 diffusion flames and annealing processing method improved the stability of gas sensors made of flame-synthesized Zn-doped γ-Fe_2O_3 particles.

5. SUMMARY AND CONCLUSION

- H_2/O_2 diffusion flame generated nanometer-sized particles; H_2/Air diffusion flame generated micrometer-sized particles.

- Optical Zn dopant concentration is 15%

- The sensors made from nanoparticles showed higher gas sensing sensitivity than sensors made of microparticles, which can be explained by surface area-volume ratio of particles.

- The sensors made of annealed particles, either micrometer-sized and nanometer-sized, did not show significant gas sensing ability.

- In the XRD analysis, deterioration of sensor ability after annealing was not because of change of crystalline structure.

- In the WH method analysis, the reduction in the signal after annealing was associated with the reduction of defects in the Zn-doped Fe_2O_3 layer.

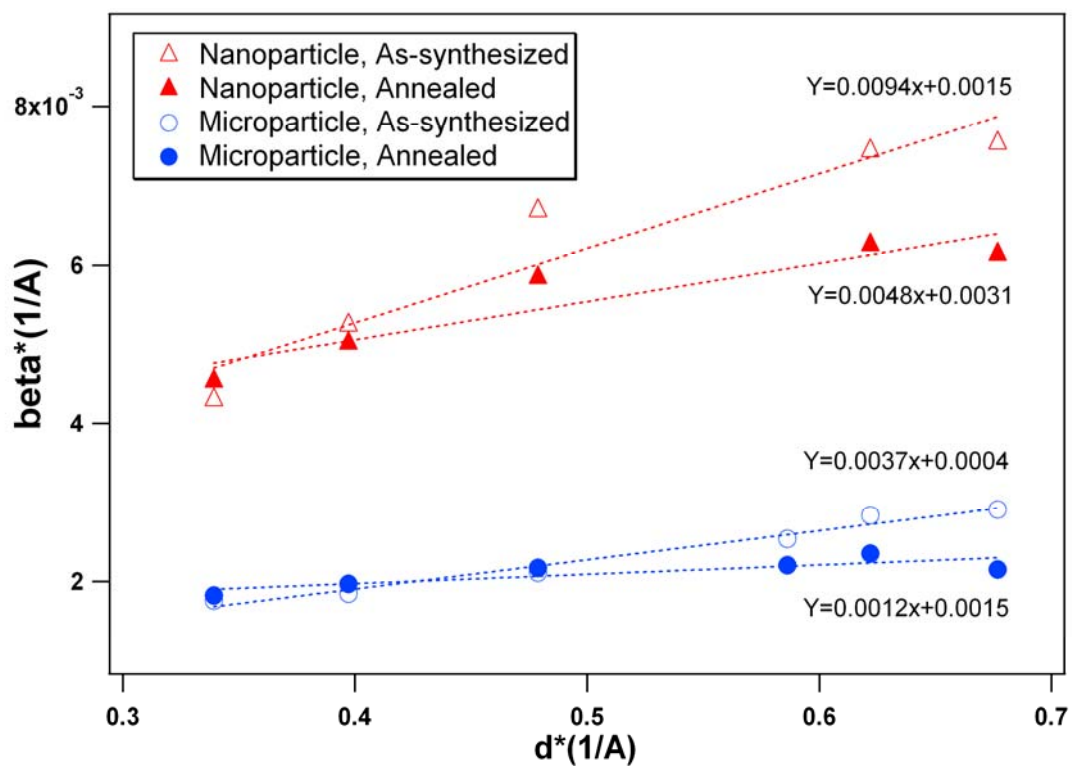- In all target gases, the sensors made of H_2/O_2 flame particles had higher stability than one made of H_2/Air flame particles.

Zn-doped Fe_2O_3 particles synthesized by flame spray pyrolysis in a high temperature flame were proved to be more effective in detecting target gases(acetone, H_2 gas) and more resistant toward aging than particles made in a low temperature flame. TEM images showed that high-temperature flame generated nanometer-sized particles. Annealing processing deteriorated the gas sensing ability, which can be explained by

WH method analysis; reduction in structural defects. However, it improved the stability of gas sensor by reducing differences of the signal between before and after aging. Therefore, the synthesis condition using H2/O2 diffusion flames and annealing process method improved the stability of gas sensors made of flame-synthesized Zn-doped γ-Fe2O3 particles

.

REFERENCES

[1] N. Barsan, D. Koziej, U. Weimar, Sensors and Actuators B-Chemical 121 (2007) 18-35.

[2] H. P. Yang, Y. F. Zhu, Biosensors & Bioelectronics 22 (2007) 2989-2993.

[3] Z. H. Jing, Materials Science and Engineering B-Solid State Materials for Advanced Technology 133 (2006) 213-217.

[4] S. W. Tao, X. Q. Liu, X. F. Chu, Y. S. Shen, Sensors and Actuators B-Chemical 61 (1999) 33-38.

[5] Z. H. Jing, Materials Letters 60 (2006) 3315-3318.

[6] Z. Jiao, S. Y. Wang, L. F. Bian, J. H. Liu, Materials Research Bulletin 35 (2000) 741-745.

[7] N. Yamazoe, Sensors and Actuators B-Chemical 5 (1991) 7-19.

[8] G. Korotcenkov, Materials Science and Engineering B-Solid State Materials for Advanced Technology 139 (2007) 1-23.

[9] M. Graf, A. Gurlo, N. Barsan, U. Weimar, A. Hierlemann, Journal of Nanoparticle Research 8 (2006) 823-839.

[10] Y. Shimizu, M. Egashira, Mrs Bulletin 24 (1999) 18-24.

[11] W. Cao, O. K. Tan, W. Zhu, B. Jiang, C. V. G. Reddy, Sensors and Actuators B-Chemical 77 (2001) 421-426.

[12] B. Guo, Z. P. Luo, Journal of the American Ceramic Society 91 (2008) 1653-1658.

[13] G. K. Williamson, W. H. Hall, Acta Metallurgica 1 (1953) 22-31.

[14] C. Z. Wu, P. Yin, X. Zhu, C. Z. OuYang, Y. Xie, Journal of Physical Chemistry B 110 (2006) 17806-17812.

[15] S. Nicoletti, L. Dori, F. Certicelli, M. Leoni, P. Scardi, Journal of the American Ceramic Society 82 (1999) 1201-1206.

[16] Z. M. Jarzebski, J. P. Marton, Journal of the Electrochemical Society 123 (1976) C199-C205.

APPENDIX A

Data for calibrated resistance to temperature curve for the RTD is shown in figure 18

and table 4.
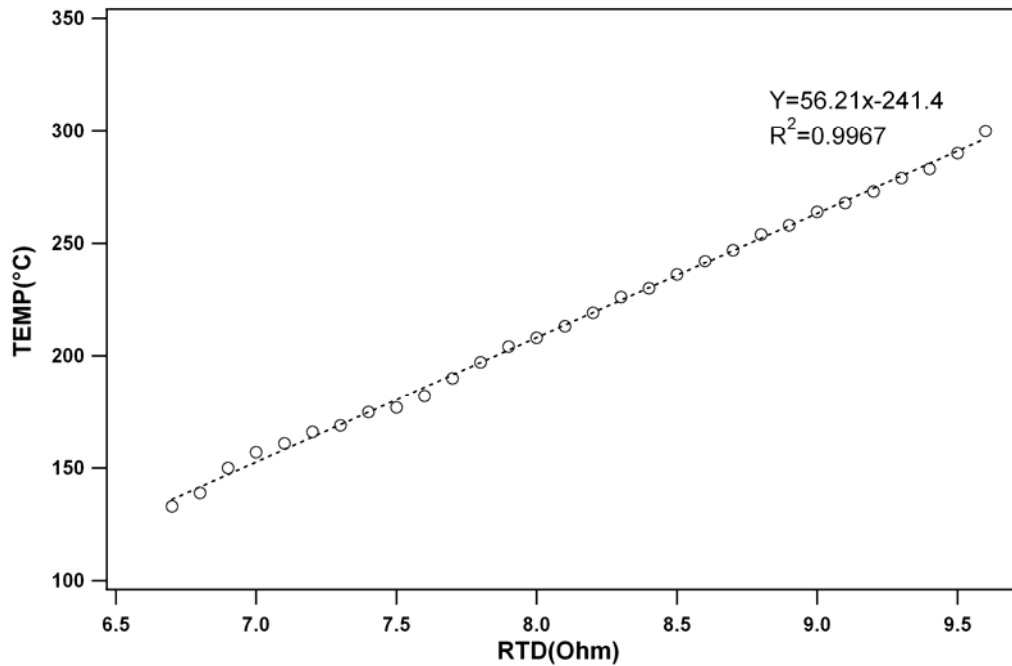
Figure 18. Graph for calibrated resistance

Table 4. Raw data of RTD plot

RTD	TEMP	ΔRTD	RTD	TEMP	ΔRTD
6.7	133	1.7	8.2	219	3.2
6.8	139	1.8	8.3	226	3.3
6.9	150	1.9	8.4	230	3.4
7	157	2	8.5	236	3.5
7.1	161	2.1	8.6	242	3.6
7.2	166	2.2	8.7	247	3.7
7.3	169	2.3	8.8	254	3.8
7.4	175	2.4	8.9	258	3.9
7.5	177	2.5	9	264	4
7.6	182	2.6	9.1	268	4.1
7.7	190	2.7	9.2	273	4.2
7.8	197	2.8	9.3	279	4.3
7.9	204	2.9	9.4	283	4.4
8	208	3	9.5	290	4.5
8.1	213	3.1	9.6	300	4.6

APPENDIX B

Nanoparticle Synthesis Procedure

Synthesize Zn doped γ-Fe2O3 in both frames (H_2/O_2 and H_2/Air) by flame spray pyrolysis apparatus. Make 30~40mg of particles for synthesizing multiple gas sensors at once.

a) Set the flame spray pyrolysis apparatus as shown in Figure 1.

b) Place the syringe containing the precursor solution on the syringe pump(Cole Parmer, Vernon Hills, IL), then set the rate of injection as 5ml/h.

c) Heat the furnace until it goes up to 500±25°C

d) Flow H_2 fuel gas and O_2 (or Air) oxidant stream at a rate of 1 SLM and 6 SLM respectively.

e) Ignite the synthesis flame at the burner nozzle.

f) Install the alumina filter (Whatman, Maidstone, England) and adjust the sampling tube on the middle of flame.

g) Feed the precursor solution into atomizer vessel by turning on the syringe pump.

h) Turning on the ultrasonic transducer to make the mist.

i) Turning on the vacuum to collect the particles on the filter.

APPENDIX C

Nanoparticle Annealing Procedure

a) Zn doped γ-Fe2O3 particles were scraped carefully off the alumina filter and put this on the glass plate.

b) Turn on the tube furnace (Barnstead International, Dubuque, Iowa). Increase the temperature at 325°C for H_2/Air flame particle and at 350°C for H_2/O_2 flame particle

c) Wait until the temperature of tube furnace has reached the desired temperature.

d) Leave the glass plate containing particles in the tube furnace for 3 days.

APPENDIX D

Sensor Aging Procedure

a) Place a gas sensor in the gas chamber. Make all the electrical connections, and make all the gas flow control connections.

b) Turn on the multimeter connected to the RTD. Read the steady state room temperature (23˚C) resistance (i.e. initial RTD).

c) Calculate the required change in RTD resistance from equation (3) to achieve the aging temperature (300˚C for H_2/Air flame particle and at 325°C for H_2/O_2 flame particle).

d) Turn on the power supply to the heater. Increase the power until the RTD resistance has reached the target RTD resistance.

e) Keep the gas sensor's heater on for 3 days in the gas chamber, while maintaining existence of ambient air

APPENDIX E

Experimental Procedure

a) Apply 1 mg of sensor material mixed with 1ml of DI water for one device.

b) Make gas sensors by applying particles on interdigitated electrodes through an aqueous solution (D.I.water) on Thermolyne$^{®}$ Type 1900 Hot Plate(Sigma – Aldrich, St.Louis, MO). Make one gas sensor with each particle type.

c) Place a gas sensor in the gas chamber. Make all the electrical connections, and make all the gas flow control connections.

d) Turn on the multimeter connected to the RTD. Read the steady state room temperature (23˚C) resistance (i.e. initial RTD).

e) Calculate the required change in RTD resistance from equation (3) to achieve the target temperature.

f) Turn on the background gas at 4 SLM (80% N_2(3.2),20% O_2(0.8)).

g) Turn on the power supply to the heater. Increase the power until the RTD resistance has reached the target RTD resistance.

h) Start reading the resistance and wait until the transient responses allow for determination of steady state conditions: the corresponding gas sensor resistance is R_b.

i) Start data of resistance acquisition from the picoammeter.

j) Turn on the target gas at a prescribed flow rate while maintaining the background gas flow rate. Measure the resistance of a gas sensor at a certain target gas concentration

k) Wait for 3 minutes and record the corresponding gas sensor resistance is R_t.

l) Turn off the target gas and wait for 10 minutes, then the resistance has reached the new R_b

m) Return to step 10) for another prescribed target gas concentration, until all the target gas concentrations have been used.

n) Leave the gas sensor's heater on for 3 days in the gas chamber, while maintaining existence of ambient air and consistent heater temperature at 300˚C for H2/Air flame (325˚C for H2/O2 flame), to age the gas sensor .Measure the resistance of the aged gas sensor with same procedures(repeat step (3) ~ (13)).

o) Leave the particles in the tube furnace, while maintaining existence of ambient air and inside furnace temperature at 325˚C for H2/Air flame (350˚C for H2/O2 flame), to anneal the particle. Measure the resistance of the annealed gas sensor with same procedures (repeat step (1) ~ (13)).

p) Repeat steps (3) – (15) until all types of gas sensors have been tested

VITA

Name: Taeyang Kim

Address: Department of Mechanical Engineering, Texas A&M University,
                 3123 TAMU, College Station, TX 77843-3123, USA

Email Address: bright1117@gmail.com

Education: B.S., Mechanical Engineering, Korea Military Academy in South
                 Korea, 2005
                 M.S., Mechanical Engineering, Texas A&M University, 2009